Gas-Phase Reactions of Nickel and Nickel-Rich Oxide Cluster Anions with Nitric Oxide. 2. The Addition of Nitric Oxide, Oxidation of Nickel Clusters, and the Formation of Nitrogen Oxide Anions

W. D. Vann, R. L. Wagner, and A. W. Castleman, Jr.*

Department of Chemistry, Pennsylvania State University, 152 Davey Laboratory, University Park, Pennsylvania 16802

Received: June 17, 1998; In Final Form: August 17, 1998

A fast flow reactor-quadrupole mass spectrometer coupled with a laser vaporization source is used to study the gas-phase reactions of nickel and nickel oxide cluster anions ($Ni_xO_y^-$, where $x = 1-12$ and $y = 0$, 1, or 2) with nitric oxide. The results indicate that three processes are occurring in the presence of the nickel cluster anions. First, nickel and nickel oxide clusters are oxidized by the reaction with nitric oxide. Second, addition products with these oxides are also formed. Third, nitrogen dioxide and nitrogen trioxide are formed on nickel oxide clusters and subsequently released as anions. Rate constants are reported for the initial reaction occurring between the nickel cluster anions and the nitric oxide, and the reaction rates are compared with reaction rates of the same nickel anion clusters with molecular oxygen. Finally, a comparison of the reaction rates for nickel oxides formed both in the flow tube and in the laser vaporization source are reported. These reactions (previously reported in Part 1[1]) help to provide a better understanding of the formation of free nitrogen oxide anions observed in the current experiments.

I. Introduction

Studying catalytic processes with cluster chemistry allows reaction processes to be studied in the gas phase where only short-range interactions between the catalyst and the reactants can take place. These systems can function as molecular scale models of localized catalytic systems. Metal[2] and metal oxide[3] clusters are often used to provide useful information on these short-range interactions occurring between a catalyst and reactant. Potential reaction mechanisms, reaction rates, competing reactions, and poisoning processes can be examined in detail with cluster chemistry. The work described in this paper is part of an ongoing investigation designed to understand these types of interactions between nickel and nickel oxide catalysts and NO_x gases.

Previously we reported[1] the reactions of nickel oxide anion clusters with nitric oxide to form nitrogen dioxide attached to the clusters. The heat of formation was dissipated by the loss of either Ni or NiO from the clusters. These reactions lead to some interesting insights into how electron density may affect local reaction centers in heterogeneous catalysts. The present study builds on the previously reported results and provides a greater understanding of heterogeneous catalytic processes that may occur between nickel catalyst and nitric oxide.

The present paper focuses on gas-phase reactions of nickel and nickel-rich oxide cluster anions ($Ni_xO_y^-$, where $x = 1-12$ and $y = 0$, 1, or 2) with nitric oxide under well-defined thermal conditions. Part 1 of this series focused on the reactions of stoichiometric to oxygen-rich nickel oxides produced by oxidizing the nickel clusters as they were being formed in the laser source. Also, the difference seen in the reaction pathways when nickel−oxygen clusters are formed in the flow tube was briefly discussed. There were some unanswered questions about these differences that will now be addressed in greater detail. To study these reactions, nickel cluster anions are produced by laser vaporization, reacted in a fast flow reactor, and then detected by a quadrupole mass spectrometer. These experiments reveal new information on reactions, reaction rates, and reaction mechanisms occurring between nickel cluster anions and nitric oxide.

II. Experimental Section

The fast flow reactor-mass spectrometer system used in this work has been described in detail previously.[4] Briefly, a nickel rod is vaporized in the presence of a flowing stream of helium carrier gas at 9000 sccm (standard cubic centimeters per minute). Water contamination is removed from the carrier gas by passing it through a series of molecular sieves in a liquid nitrogen bath. The continuous flow of helium carries the ablation species out of the source through a conical nozzle into the flow tube. Laser vaporization is performed using the second harmonic of a Nd:YAG laser focused onto a 0.6-cm rotating nickel rod by a 20-cm focal length lens.

As the ions are carried through the flow tube, they are thermalized (296 K) by collisions with the carrier gas. The flow tube pressure is maintained at around 300 mTorr. To study the reactions of interest, neutral reactant gases are added through a reactant gas inlet. The reactant ions are allowed to react in the flow tube for a measured amount of time before they are sampled and detected. The majority of the species flowing through the reaction region are pumped off by a high volume roots pump, while a fraction of the ions is sampled from the flow through a 750-μm orifice and focused into the quadrupole mass filter by a set of electrostatic lenses. Thereafter, the ions are detected by a channel electron multiplier. The quadrupole mass filter is controlled by an Extrel mass controller. The quadrupole and detection chambers are differentially pumped, with pressures maintained around 10^{-5} Torr. The pulsed output from the multiplier is fed through a pulse amplifier discriminator and then to a computerized multichannel analyzer.

10.1021/jp982673y CCC: $15.00
Published on Web 10/09/1998

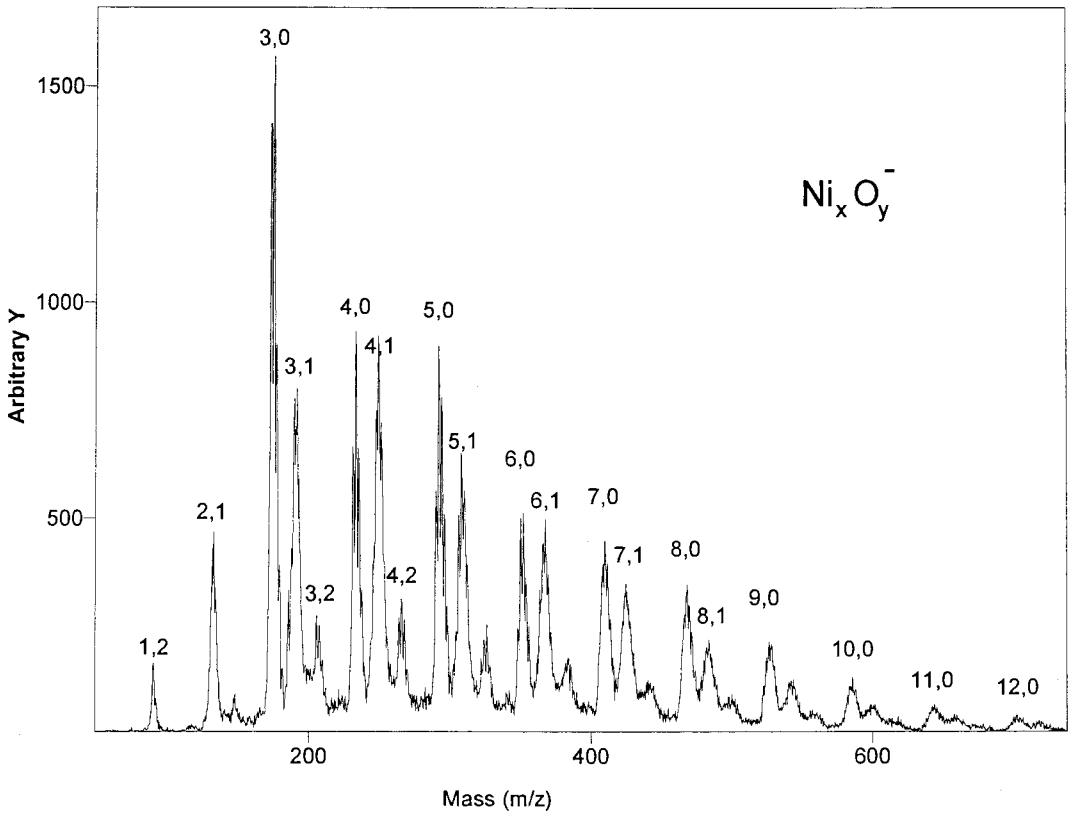

Figure 1. Typical nickel anion cluster distribution.

III. Results

Nickel and nickel-rich oxide cluster anions are formed by laser vaporization of a nickel rod. A typical nickel and nickel rich oxide anion cluster distribution is given in Figure 1. The major peaks in the spectrum are labeled as $Ni_xO_y^-$. The most prominent peak in the spectrum is the nickel trimer, and the next two most abundant clusters are the nickel pentamer and tetramer. The presence of nickel oxides in this distribution indicates how easily bare nickel anions are oxidized. There was no oxygen intentionally added to the flow tube. Oxides are present in and on the nickel rod itself and/or from minute leakage of air into the apparatus. To reduce the amount of oxides in the distribution, the nickel rod can be ablated for several hours to remove oxides from the surface of the rod; also, lowering the laser fluence helps to reduce oxidation. The typical laser fluence for vaporization/ionization of the nickel rod is 4 to 5 mJ.

Nitric oxide was reacted with different nickel/nickel oxide cluster anion distributions such as the distribution shown in Figure 1. Different reaction product distributions were obtained by varying the concentration of nitric oxide and by varying the nickel cluster reactant distributions. Two product distributions for the reaction of nitric oxide with nickel/nickel oxide cluster anions (Figure 1) are given in Figure 2. The identification of product species is given careful consideration. Both individual isotope patterns and overall product buildup distributions are painstakingly considered when assigning product distributions. These and other procedures for identifying product species are explained extensively in Part 1 of this series.[1]

The lower spectrum shown in Figure 2 is for a low NO concentration (0.2 sccm) and the upper spectrum is for a higher concentration (2.0 sccm). The product species are labeled as $Ni_xO_y(NO)_z^-$ and the starting materials remaining at this concentration are labeled as $Ni_xO_y^-$. There are, however, two exceptions, the NiO_2^- and $Ni_3O_2^-$ oxides are not completely due to starting material; rather, they are partially due to the formation of these species as products. As shown later, nickel oxides are a major product in these reactions; however, in this particular product distribution, these are the only two species showing an increase in ion concentration from the nickel oxide starting materials.

Another major product of this reaction is the addition of nitric oxide to the nickel oxide clusters. Figure 2 shows three such products as the reaction begins at the lowest concentration of nitric oxide. These are indicated by the dashed lines, and are the $Ni_3O(NO)^-$, $Ni_4O(NO)^-$, and $Ni_5O(NO)^-$ clusters. Also the higher concentration spectrum in Figure 2 (top) shows several other addition products as the reaction progresses. It is important to note that there are no additions of NO to any bare nickel cluster anions (Ni_x^-), and this holds true throughout all data sets that were obtained in these experiments.

There are also many nitric oxide addition products that are attached to nickel oxide species that were not present in such high concentrations in the starting material. For instance, even if the association process is an efficient one, there was insufficient $Ni_4O_2^-$ starting material to form the large abundance of $Ni_4O_2(NO)^-$ cluster. This species is a dominant product in the higher concentration product distribution in Figure 2. This can be illustrated by plotting the change in intensities of these species (starting material, $Ni_4^-Ni_4O^-$, and $Ni_4O_2^-$, and products $Ni_4O_2NO^-$, $Ni_4O(NO)_3^-$) as shown in Figure 3, where the three nickel tetramer reactants are seen to decrease as the two tetramer products increase. The intensities of the $Ni_4O_2(NO)^-$ cluster were determined by subtracting out any contribution due to the fourth isotope of the nickel pentamer (296 amu), which overlaps with the main isotope of this product (296 amu) and was large at low concentrations. The same procedure was used on the $Ni_4O(NO)_3^-$ product to remove any contribution from the Ni_5O

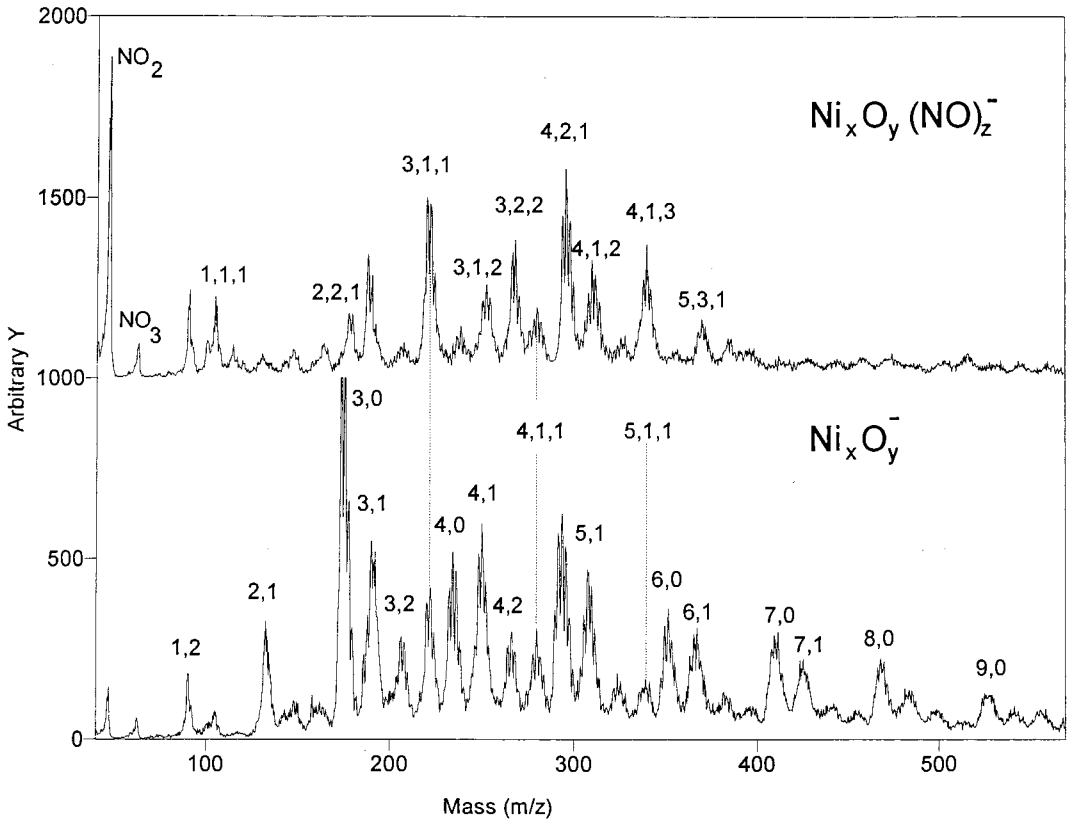

Figure 2. Two nitric oxide reaction product distributions. The bottom spectrum is for 0.2 sccm of NO and the top spectrum is for 2.0 sccm of NO. The three dashed lines indicate the first reaction products observed for the trimer, tetramer, and pentamer clusters.

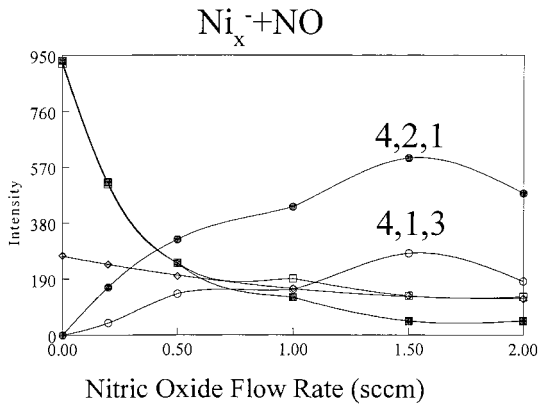

Figure 3. Relative anion concentration of nickel tetramer reactants and products. Key: (■) indicates Ni_4^-; (□) Ni_4O^-; (◆) $Ni_4O_2^-$; (●) $Ni_4O_2NO^-$; (○) $Ni_4O(NO)_3^-$.

cluster. This was accomplished simply by knowing the isotopic ratios of the nickel pentamer clusters and determining the contribution of the fourth isotope based on the intensities of other isotopes that do not overlap with any product material. In Figure 3 the filled diamonds represent the Ni_4O_2 cluster, and it is obvious that the decrease in intensity of this cluster cannot account for the increase in intensity of the $Ni_4O_2(NO)^-$ cluster (filled circles). Therefore, the Ni_4O (open squares) or Ni_4 (filled squares) reactants must be also contributing to the formation of $Ni_4O_2(NO)^-$ clusters. Likewise, the decrease in intensity of the Ni_4O cluster cannot account for the increase in the combined intensities of the $Ni_4O_2(NO)^-$ and $Ni_4O(NO)_3^-$ (open circles) clusters, and this does not even take into consideration the $Ni_4O(NO)_2^-$ cluster. These observations indicate that at least the Ni_4 and possibly the Ni_4O cluster are being oxidized by the nitric oxide. It is possible that larger nickel clusters may also be involved in these reactions through fragmentation processes, however the main point is that nickel clusters with increased oxygen contents are formed.

Oxidation of the nickel clusters can be further seen in Figure 4 where the reactions of nitric oxide can be followed as a function of its concentration. This is a different data set from those shown thus far. The dashed lines indicate the oxidation of the cluster and the solid lines indicate the addition of nitric oxide. The bottom spectrum displays the reactants $Ni_xO_y^-$, where y is 0, 1, or 2. This distribution has a greater percentage of the nickel monoxide and dioxide reactants than are reacted to produce the data set shown in Figures 1 and 2. The next spectrum up in Figure 4 was obtained at 0.2 sccm of NO, and shows the formation of higher nickel oxides, namely, $Ni_2O_3^-$, $Ni_3O_3^-$, $Ni_4O_3^-$, and some $Ni_4O_4^-$. The third spectrum up in Figure 4 is at 0.4 sccm of NO, where further oxidation of the nickel trimer and tetramer are seen to contribute to the formation of $Ni_3O_4^-$, and $Ni_4O_4^-$. At this concentration, addition of nitric oxide onto the clusters is observed, with the formation of the $Ni_3O_4(NO)^-$, $Ni_4O_3(NO)^-$, and $Ni_4O_3(NO)_2^-$ clusters. The next three spectra were obtained at increasing concentrations of nitric oxide (0.6, 0.8, and 1.0 sccm), and continue to show both further oxidation of the nickel oxide clusters and addition of NO onto these clusters. In another set of data, larger nickel cluster reactants were looked at more closely and were found to react in a similar fashion. For instance, the Ni_8^- cluster was observed to oxidize up to $Ni_8O_6^-$ and also to form addition products such as $Ni_8O(NO)^-$, $Ni_8O_2(NO)^-$, and $Ni_8O_2(NO)_2$.

The third type of major products from these reactions are nitrogen dioxide (NO_2^-) and nitrogen trioxide (NO_3^-) anions, as well as some further clustering of these species when very high concentrations of nitric oxide are added. The higher concentration product distribution in Figure 2 clearly shows the

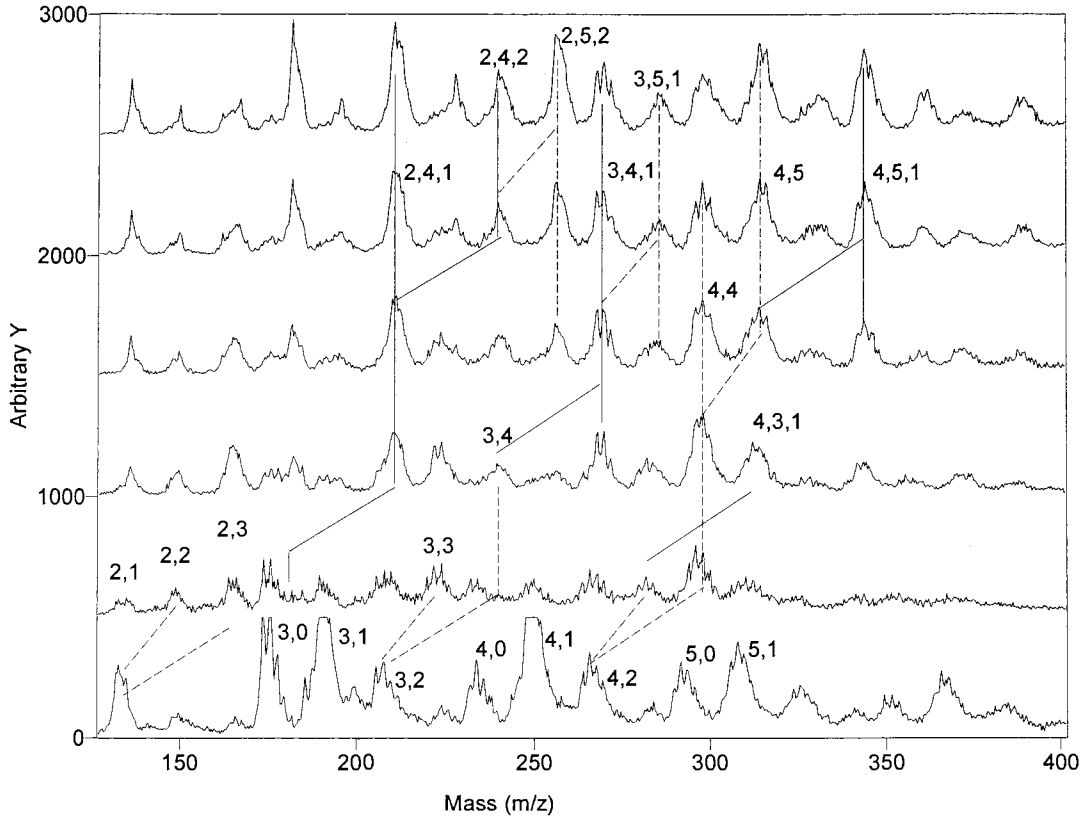

Figure 4. Oxidation and addition reactions of nickel anion cluster from the addition of increasing concentrations of nitric oxide (from bottom to top: 0, 0.2, 0.4, 0.6, 0.8, and 1.0 sccm).

formation of these two species. An interesting difference in the formation of these NO_x^- products is observed between the two different data sets discussed thus far (Figures 2 and 4). The distributions taken at the lowest NO concentrations in both Figures 2 and 4 are each for the same concentration of NO and yet lead to different products. The key to understanding this difference is to carefully compare each of the nickel/nickel oxide reactant spectra and then to see how the two reactant distributions produce different products. This comparison is made in Figure 5, where the two reactant spectra are overlaid at the bottom of the figure and slightly offset for clarity. The two product spectra are also shown overlaid and offset at the top of the figure. The main difference in the reactant spectra (bottom) is that one has significantly less bare nickel species and therefore has a greater relative amount of nickel oxides. The most striking difference, however, is in the product distributions, where the relative rate of formation of NO_2^- and NO_3^- at this same concentration is significantly faster for the data set with the dominate oxide species.

One final observation from the data is that in all data sets, the only initial nickel monomer reactant present was NiO_2^-, and, as mentioned previously, this species increased with increasing NO concentration. Other subsequent nickel monomer products were $NiO_3(NO)^-$, $NiO_2(NO)_2^-$, $NiO_3(NO)_2^-$, $NiO_4(NO)_2^-$, and $NiO_3(NO)_3^-$. In one set of data, the NiO_2^- intensity at 1 sccm of NO was about 2 times the initial intensity with no NO addition. The $NiO_4(NO)_2^-$ cluster was found to be approximately twice the intensity of the initial NiO_2^- signal, and the remaining monomer products when combined were around 3 times the initial NiO_2^- intensity. These data indicate that the nickel monomer product species are coming from higher nickel reactants.

In a series of experiments to elucidate the reaction rates, both nitric oxide and molecular oxygen were reacted with distributions such as that shown in Figure 1. Determination of the pseudo-first-order bimolecular rate constants for the reaction:

$$Ni_x^- + NO \rightarrow\rightarrow Ni_xO_y(NO)_z^- + \text{neutrals} \qquad (1)$$

is obtained from the slope of a semilog plot through the following relation

$$\ln(I/I_o) = -k[NO]t \qquad (2)$$

where I/I_o is the intensity of the Ni_x^- species at given concentration of NO divided the intensity of the Ni_x^- species at zero concentration, k is the rate constant, and t is the reaction time (4.2 ms measured by pulsing experiments[5]). Examples of the semilog plots used to determine rate constants for each of the reactions carried out in these experiments are given in Figure 6. For each reaction spectra at a given concentration, one or more reference spectra (i.e. zero concentration spectra) are taken.

The reaction rates for the reactions given in Tables 1−4 were determined by averaging several different data sets to eliminate scan-to-scan fluctuations in the data. Some reaction products overlap with starting material, but often these reaction rates were able to be obtained from a measurement of the changing concentration of starting material isotopes that did not have mass overlap. All reaction rates that could be obtained without interference from product overlap are reported in Tables 1−4, and are given in cm^3/s. The larger errors reported in some reaction rates are attributable in part to product mass overlap, reducing the usable data points. Also, lower concentrations of starting material of the larger clusters contributed to these errors. In addition to reaction rates, calculated collision rates (Langevin limit for nonpolar molecules and Su-Chesnavich parametrization for polar molecules[6]) are provided in each table. A comparison

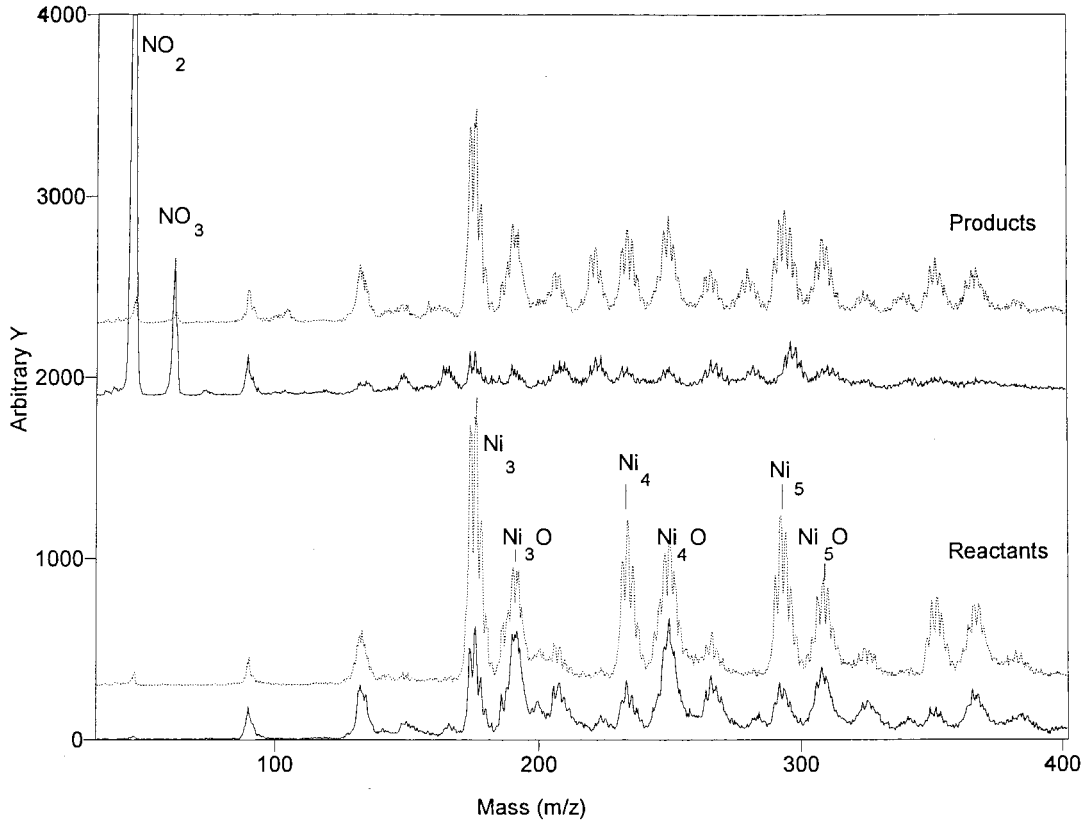

Figure 5. A comparison of reactants and products with two different data sets. The dashed-lined spectra are reactant and product distributions for the data set shown in Figure 2 and the solid-lined spectra are for the data set shown in Figure 4.

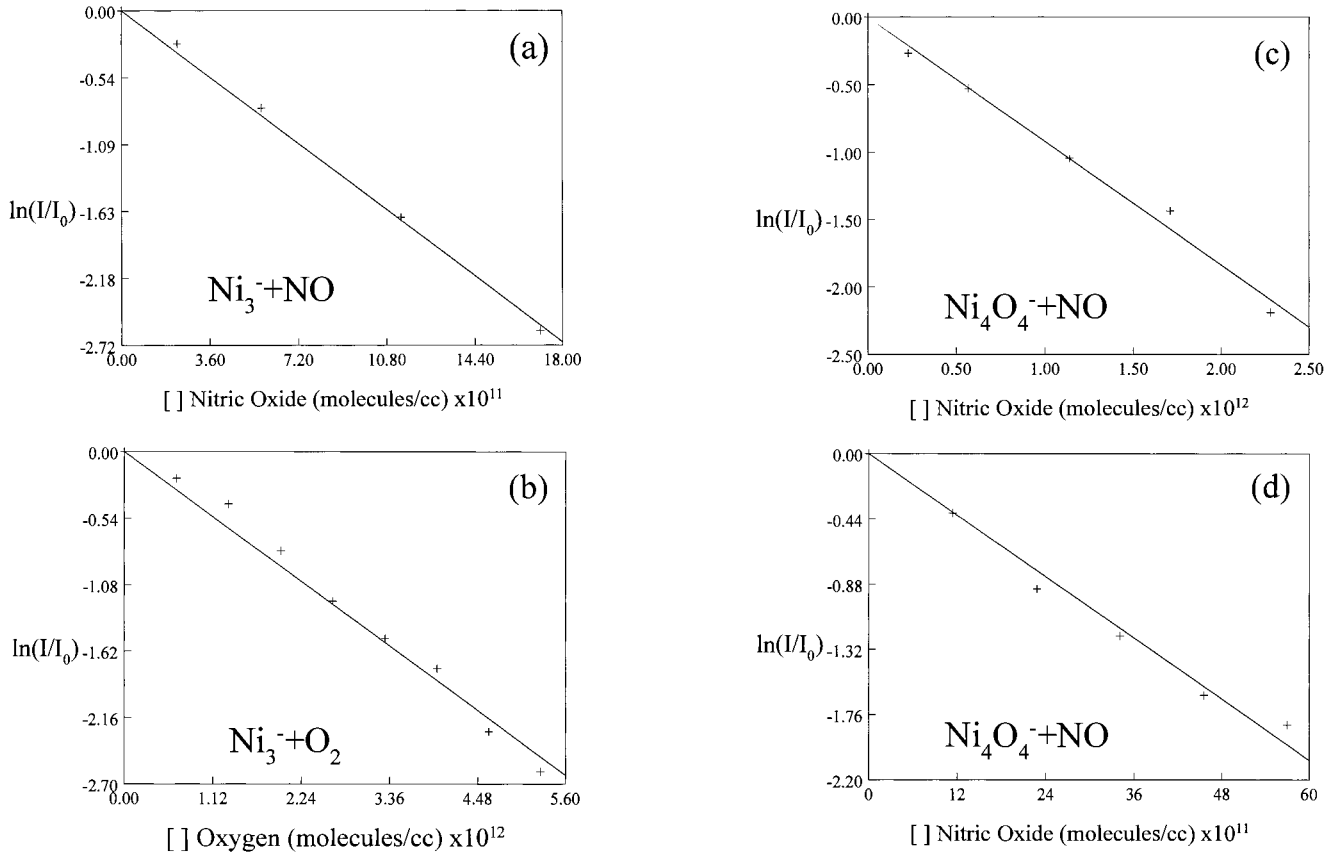

Figure 6. Examples of semilog plots for rate constant determination. (a) $Ni_3^- + NO$; (b) $Ni_3^- + O_2$; (c) $Ni_4O_4^-$ (formed in the flow tube) + NO; and (d) $Ni_4O_4^-$ (formed in the laser vaporization source) + NO.

of these collision rates with the experimentally determined rates gives an indication of the efficiency of the reactions. The reaction rates of nitric oxide reaction with nickel clusters anions are given in Table 1.

TABLE 1: NO Reactions with Nickel Cluster Anions

reaction	experimental rate constants (10^{-10}cm^{3}s^{-1})	calculated collision rates (10^{-9}cm^{3}s^{-1})
$Ni_3^- + NO \rightarrow \rightarrow Ni_3O_x(NO)_y^-$	3.09 ± 0.28	1.55
$Ni_4^- + NO \rightarrow \rightarrow Ni_4O_x(NO)_y^-$	4.32 ± 0.19	1.52
$Ni_5^- + NO \rightarrow \rightarrow Ni_5O_x(NO)_y^-$	4.12 ± 0.19	1.51
$Ni_6^- + NO \rightarrow \rightarrow Ni_6O_x(NO)_y^-$	3.60 ± 0.24	1.49
$Ni_7^- + NO \rightarrow \rightarrow Ni_7O_x(NO)_y^-$	4.13 ± 0.39	1.49
$Ni_8^- + NO \rightarrow \rightarrow Ni_8O_x(NO)_y^-$	4.24 ± 0.33	1.48
$Ni_9^- + NO \rightarrow \rightarrow Ni_9O_x(NO)_y^-$	3.61 ± 0.61	1.47
$Ni_{10}^- + NO \rightarrow \rightarrow Ni_{10}O_x(NO)_y^-$	2.39 ± 0.25	1.47
$Ni_3O^- + NO \rightarrow \rightarrow Ni_3O_x(NO)_y^-$	$\leq 3.67 \pm 0.16$	1.54
$Ni_4O^- + NO \rightarrow \rightarrow Ni_4O_x(NO)_y^-$	$\leq 3.15 \pm 0.36$	1.52
$Ni_5O^- + NO \rightarrow \rightarrow Ni_5O_x(NO)_y^-$	$\leq 2.55 \pm 0.26$	1.50
$Ni_6O^- + NO \rightarrow \rightarrow Ni_6O_x(NO)_y^-$	$\leq 3.61 \pm 0.25$	1.49
$Ni_7O^- + NO \rightarrow \rightarrow Ni_7O_x(NO)_y^-$	$\leq 3.08 \pm 0.37$	1.48

TABLE 2: Oxygen Reaction Rates

reaction	experimental rate constants (10^{-10}cm^{3}s^{-1})	calculated collision rates (10^{-10}cm^{3}s^{-1})	previously published rate constants[7] (10^{-10}cm^{3}s^{-1})
$Ni_3^- + O_2 \rightarrow Ni_3O_x^-$	1.12 ± 0.08	5.66	0.78 ± 0.02
$Ni_4^- + O_2 \rightarrow Ni_4O_x^-$	3.01 ± 0.43	5.55	3.4 ± 0.3
$Ni_5^- + O_2 \rightarrow Ni_5O_x^-$	2.98 ± 0.15	5.48	3.1 ± 0.3
$Ni_6^- + O_2 \rightarrow Ni_6O_x^-$	1.91 ± 0.16	5.43	2.2 ± 0.1
$Ni_7^- + O_2 \rightarrow Ni_7O_x^-$	2.53 ± 0.28	5.40	3.0 ± 0.3
$Ni_8^- + O_2 \rightarrow Ni_8O_x^-$	2.49 ± 0.26	5.38	2.8 ± 0.3
$Ni_9^- + O_2 \rightarrow Ni_9O_x^-$	2.44 ± 0.18	5.36	2.4 ± 0.4
$Ni_{10}^- + O_2 \rightarrow Ni_{10}O_x^-$	3.19 ± 0.45	5.34	3.8 ± 1.3
$Ni_{11}^- + O_2 \rightarrow Ni_{10}O_x^-$	4.39 ± 0.36	5.33	
$Ni_{12}^- + O_2 \rightarrow Ni_{10}O_x^-$	4.06 ± 0.38	5.32	
$Ni_{13}^- + O_2 \rightarrow Ni_{10}O_x^-$	4.12 ± 0.26	5.31	
$Ni_{14}^- + O_2 \rightarrow Ni_{10}O_x^-$	2.4 ± 0.7	5.30	
$Ni_{15}^- + O_2 \rightarrow Ni_{10}O_x^-$	2.7 ± 1.0	5.30	

TABLE 3: NO Reactions with Nickel Oxide Cluster Anions (Flow Tube) to Form Addition Products

reaction	experimental rate constants (10^{-10}cm^{3}s^{-1})	calculated collision rates (10^{-9}cm^{3}s^{-1})
$Ni_3O_3^- + NO \rightarrow Ni_xO_yNO_z^-$	2.86 ± 0.20	1.53
$Ni_4O_4^- + NO \rightarrow Ni_xO_yNO_z^-$	4.21 ± 0.19	1.50
$Ni_6O_7^- + NO \rightarrow Ni_xO_yNO_z^-$	2.09 ± 0.20	1.48
$Ni_7O_6^- + NO \rightarrow Ni_xO_yNO_z^-$	6.07 ± 0.40	1.47

TABLE 4: NO Reactions with Nickel Oxide Cluster Anions (Source) to Form NO_2

reaction	experimental rate constants (10^{-10}cm^{3}s^{-1})	calculated collision rates (10^{-9}cm^{3}s^{-1})
$Ni_4O_4^- + NO \rightarrow Ni_xO_y(NO_2)_z^-$	0.51 ± 0.10	1.50
$Ni_4O_5^- + NO \rightarrow Ni_xO_y(NO_2)_z^-$	1.2 ± 0.3	1.50
$Ni_5O_5^- + NO \rightarrow Ni_xO_y(NO_2)_z^-$	0.37 ± 0.13	1.49
$Ni_5O_6^- + NO \rightarrow Ni_xO_y(NO_2)_z^-$	7.1 ± 2.9	1.49
$Ni_6O_6^- + NO \rightarrow Ni_xO_y(NO_2)_z^-$	0.37 ± 0.06	1.48
$Ni_6O_7^- + NO \rightarrow Ni_xO_y(NO_2)_z^-$	0.52 ± 0.10	1.48

It is interesting to compare the reaction rates in Table 1 with those of oxygen with nickel cluster anions in Table 2. Rate constants for the reaction of nickel anions with oxygen were recently published by Hintz and Ervin[7] for Ni_3^- to Ni_{10}^- and are provided for a comparison, in general showing good agreement. Further, new rate constants for the reactions of Ni_{11}^- to Ni_{15}^- with oxygen are also given in Table 2. Also, thus far unpublished reaction rates of several different nickel oxide anions from previous experiments[1] in our laboratory are given to illustrate the large difference in reaction rates between nickel oxides formed in the source and those formed in the flow tube. These rates are listed in Tables 3 and 4, where only those reaction rates that are not affected by product overlap are listed.

IV. Discussion

The study of reactions of nitric oxide with nickel cluster anions yields some interesting results. There are at least three different processes occurring with the reaction of NO. First, the addition of NO with the nickel and nickel oxide clusters, then oxidation of both nickel and nickel oxide clusters, and finally the oxidation of NO to form NO_2^- and NO_3^-. Although only the nickel oxide addition species are observed in the mass spectra, bare nickel addition species must be an intermediate product in the oxidation reactions. One would expect that NO adds to the nickel clusters and is quickly reduced releasing nitrogen. Although no product anion is observed with the addition of nitrogen atoms, it is reasonable to assume that nitrogen quickly reacts with NO to form N_2O. The N_2O would not be expected to be observed as an ion from this reaction because of its low electron affinity compared with NO_2 and nickel/nickel oxide clusters.[8] All product spectra were checked for the presence of N_2O either as a molecular ion or as part of a cluster and no evidence of N_2O was found.

The fact that the $Ni_xO(NO)^-$ clusters are the first addition species seen in the spectra and that no $Ni_x(NO)^-$ species are observed indicates that the oxidation process slows or at least becomes comparable to the rate of association after one oxygen is attached to the cluster. Surface studies show that when NO is added to nickel surfaces, NO adsorbs to the surface, followed by dissociation depending on surface coverage (NO concentration) and finally N_2 is desorbed.[9] However, this formation of N_2 on transition metal surfaces occurs through a Langmiur−Hinshelwood process, where two adsorbates (either N(a) + N(a) or N(a) + NO(a)) react to form the product (N_2).[9−11] Although there is a possibility that such a process may occur on the surface of some of the clusters in the reactant distributions, it is not likely that it occurs on bare metal nickel clusters. For this mechanism to proceed it would be necessary to first form Ni_x-NO species, none of which are observed in any product distribution. The formation of Ni_xO^- species (the first product observed from a bare metal cluster) is also taken into consideration when reporting the reaction rates for $Ni_xO^- + NO$ (Table 1), and subsequently reported only as a lower limit for the rate constants.

The most striking species seen in the mass spectra is the formation of NO_2^- from the addition of NO to the nickel\nickel oxide clusters. Also, NO_3^- is a product. There is obviously the reduction of NO to form nickel oxides but these oxides, once formed, have the opposite effect on the nitric oxide, that is, they oxidize the nitric oxide. When the reactant distribution contains more nickel oxide species, the rate of NO_2^- formation dramatically increases, as is shown in Figure 5. This fact would indicate that the formation process is occurring on the nickel oxide clusters and not the bare nickel clusters. When oxygen was added to the flow tube to form nickel oxides in a previous experiment,[1] one of the products formed was NO_2^-. This product was thought simply to be due to the reaction of nitric oxide with the excess oxygen in the flow tube. However, the fact that excess oxygen did not react to form NO_2^- when oxygen was added at the laser vaporization source, where high-temperature conditions produced oxides of greater stability, was unexplained. It is now believed that the formation of NO_2^- occurs by a reaction involving clusters. One consideration was whether the elimination of electrons by some scavenging reaction with the nickel oxides produced in the source could have prevented the formation of NO_2^- as a product; but if oxides

depleted electrons at the source, they would have depleted them when formed in the flow tube as well. The appearance of NO_2^- and NO_3^- when no excess oxygen is present in the flow tube and the fact that the primary reaction that occurs between NO and the nickel clusters is the oxidation of the nickel clusters indicate that very similar processes are occurring in both experiments. That is, weakly bound nickel oxides, once formed either by reactions of nickel clusters with oxygen or nitric oxide, contribute to the formation of nitrogen dioxide in the presence of nitric oxide. The fact that nickel oxides produced in the laser vaporization source form nitrogen dioxide on the nickel oxide cluster but not as a free ion is another indication that the bonding with these oxides is stronger than with those formed in the flow tube.

Much can be learned about these reactions by looking carefully at the kinetic data and by comparing these reaction rates. For instance, there is obviously a different reaction process occurring when oxides are made in the laser vaporization source compared with those made in the flow tube. A comparison of the reaction rates shows a significant difference between these two reactant distributions with nitric oxide. The reaction rate of $Ni_6O_7^-$ with NO is 4 times faster for oxides formed in the flow tube (Tables 3 and 4). Also observed (for the $Ni_4O_y^-$ and $Ni_5O_y^-$) is a significant slowing of the NO_2 formation mechanism for clusters of stoichiometric oxide (1:1) compositions, indicating that the presence of excess oxygen on the cluster helps the reaction to proceed faster (Table 4). Comparing the Ni_3^- and Ni_4^- (Table 1) reaction rates with the $Ni_3O_3^-$ and $Ni_4O_4^-$ (Table 3) rates shows that the bare nickel clusters tend to react slightly faster than the oxides. This difference in reaction rates agrees with what is observed for bulk reactions and may indicate that the addition of nitric oxide occurs faster for the bare nickel than for nickel oxide clusters. Reactions of both nickel and rhodium surfaces show that dissociative NO chemisorption is largely suppressed by adsorbed oxygen.[9,12] It is also interesting to note that NO has a faster reaction rate than O_2 with bare nickel anion clusters (Tables 1 and 2), indicating that the oxidation process is faster with NO than with O_2. This result is, however, consistent with calculated collision rates as reported in Tables 1 and 2, where nitric oxide would have a greater capture cross section because of its' dipole moment.

The considerably slower rate reported for the reaction of the nickel trimer with oxygen explains the prominence of the nickel trimer in Figure 1. The other species seen in this distribution show only subtle differences. The most noticeable of these subtleties is found in the Ni_4O^- and the Ni_6O^- species. The ratio of these two oxides to their respective bare metal species is considerably larger. It was mentioned earlier that the amount of oxides in the spectra decreases the longer the rod is ablated, which suggests that oxides are being removed from the surface of the rod. As the ratio of oxides to their respective bare metal species decreases, the ratio Ni_4O^- to Ni_4^- and of Ni_6O^- to Ni_6^- decreases at a noticeably slower rate than the other nickel species. This result suggests that Ni_4O^- and Ni_6O^- are more stable than the other oxides seen in the distribution. Further, Ni_7O^- was intermediately reactive between these two species (Ni_4O^- and Ni_6O^-) and the other oxides. Finally, the rate limits reported for the Ni_xO species are slower than the actual rates. This slowing of the rate constants is due to the simultaneous formation of Ni_xO^- while the depletion of these species is being measured.

It was suggested in Part 1 that nickel−oxygen clusters formed in the flow tube may have greater oxygen content toward the outside of the clusters due to their formation mechanism. This arrangement was suggested to lead to the bonding of nitric oxide to oxygen as opposed to nickel, which would then facilitate the formation of nitrogen dioxide on the cluster without the loss of any nickel species from the cluster. It is then reasonable to expect that the formation of NO_2^- as a product could come from this formation of NO_2 on the nickel oxide cluster and that the heat of formation would cause the loss of NO_2^- from the cluster instead of Ni or NiO as was seen in Part 1. Perhaps very similar processes are actually occurring in each case; that is, both form NO_2 on the nickel oxide clusters, both dissipate the heat of formation by the loss of some species from the cluster (either Ni, NiO, or NO_2), and both show some indication of NO addition species.

The NO addition species and mixed NO addition/NO_2 formation species cannot in all cases be distinguished from the formation of NO_2 on the cluster. Obviously, the addition of NO on the cluster is an intermediate for the formation of NO_2, but it is difficult to say exactly which species are NO_2 and which are NO with O attached to nickel. It is possible that there may be some NO_2 attached to the clusters, especially if one considers that for nickel oxide clusters that are richer in nickel, some of the oxygen involved in the formation of NO_2 may be more strongly bound to the cluster. This possibility would make sense both because of the propensity of nickel to oxidize at the point of laser vaporization (which forms more strongly bound oxides) and the fact that the nickel oxide clusters that formed clusters with greater oxygen content (as discussed in Figures 4 and 5) produced NO_2^- at a significantly faster rate. It was suggested in Part 1 of this series that the reason NO_2 was not formed on (and remained attached to) the surface of the cluster was because of the difference between the nickel−oxygen bonding of two types of oxide clusters. With oxygen intricately and strongly bound to the nickel in the cluster, NO_2 was formed attached to the cluster, and Ni or NiO was lost to dissipate the heat of formation. With oxygen less strongly bound and more accessible to the cluster surface, NO_2 was also formed. However, the oxygen involved in the formation of NO_2 could more easily be removed from the cluster to form NO_2^- as a free ion. Considering these two mechanisms, it is conceivable that the more intricately bonded oxygen of a nickel oxide cluster would react somewhat slower, which is consistent with the reaction rates measured for these two processes.

Next, consider the indication that nickel monomer cluster species are products of higher nickel oxide clusters. Perhaps this indication can be explained by the breaking apart of the nickel oxide cluster itself caused by the heat of formation of the NO_2 on the more weakly bound clusters. This process would suggest that the oxygen, when more thoroughly incorporated into the cluster, acts to stabilize the cluster. There was no evidence of fragmentation in nickel oxides formed in the high-temperature process of oxidation that occurred in the laser vaporization source. This result then provides further evidence that the bonding in these clusters, as has been suggested, is considerably stronger when compared to the bonding of oxygen to the room-temperature nickel clusters. With this result in mind, it is possible that the oxygen that is bound to the nickel-rich clusters prior to the reaction with nitric oxide is more strongly bound because it is added by reactions occurring in the laser vaporization source. This stronger binding may account for the formation of nickel monomer loss channels. Also, the faster rate of formation of NO_2^- by the more oxygen-rich nickel oxide clusters (Figure 4) could be a function of having some strongly bound oxygen (initial oxygens) and some more weakly bound oxygen (from further oxidation by NO

reactions), suggesting that the oxygen added by reactions with nitric oxide becomes more and more weakly bound as the oxygen content of the cluster increases.

V. Conclusion

The reactions of nitric oxide with nickel and nickel oxide cluster anions cause the formation of nitrogen dioxide and the subsequent loss of species from the cluster to dissipate the heat of formation. In Part 1 of this series, the loss of Ni or NiO from the cluster was observed when strongly bound nickel oxides were formed in the laser vaporization process. When less strongly bound nickel oxide clusters were formed by reacting oxygen with room-temperature nickel clusters, the formation of nitrogen dioxide was observed by the loss of NO_2^- from the cluster. The reaction of nitric oxide with nickel cluster anions initially reduces the nitric oxide and forms nickel oxide clusters. These nickel oxide clusters are rich in nickel. The nickel-rich oxide clusters then react with the nitric oxide to form nitrogen dioxide, and the heat of formation is again dissipated by loss of species from the cluster, in this case, both NO_2^- and nickel monomer species are the loss products. It is possible that the oxygen that is bound to the nickel-rich clusters prior to the reaction with nitric oxide is more strongly bound because it is added by reactions occurring in the laser vaporization source. This stronger binding may account for the formation of nickel monomer loss channels.

Acknowledgment. Funding provided by the Department of Energy, grant # DE-FG02-92ER14258, is gratefully acknowledged.

References and Notes

(1) Vann, W. D.; Wagner, R. L.; Castleman, A. W., Jr. *J. Phys. Chem.* **1998**, *102*, 1708.

(2) (a) Riley, S. E. In *Metal Ligand Interactions: From Atoms, to Clusters, to Surfaces*; Salahub, D. R., Russo, N., Eds.; Kluwer Academic: Dordrecht, 1992; pp 17−36. (b) Eller, K.; Schwarz, H. *Chem. Rev.* **1991**, *91*, 1121.

(3) (a) Fialko, E. F.; Kikhtenko, A. V.; Goncharov, V. B.; Zararaev, K. I. *J. Phys. Chem.* **1997**, *101*, 5772. (b) Shröder, D.; Schwarz, H. *Angew. Chem., Int. Ed. Engl.* **1995**, *34*, 1973.

(4) Castleman, A. W., Jr.; Weil, K. G.; Sigsworth, S. W.; Leuchtner, R. E.; Keesee, R. G. *J. Chem. Phys.* **1987**, *86*, 3829.

(5) (a) Pulsing experiments are conducted by interrupting a continuous signal with an electrical pulse at the reactant gas inlet and the sampling orifice. The time difference measured between these two interruptions is the residence time of ions in the reaction zone, under those experimental conditions. (b) MacTaylor, R. S.; Vann, W. D.; Castleman, A. W., Jr. *J. Phys. Chem.* **1996**, *100*, 5329.

(6) Mackay, G. I.; Betowski, L. D.; Payzant, J. D.; Schiff, H. I.; Bohme, D. K. *J. Phys. Chem.* **1976**, *80*, 2919; Su, T.; Chesnavich, W. J. *J. Chem. Phys.* **1982**, *76*, 5183.

(7) Hintz, P. A.; Ervin, K. E. *J. Chem. Phys.* **1995**, *103*, 7897.

(8) (a) Ervin, K. E.; Ho, J.; Lineberger, W. C. *J. Phys. Chem.* **1988**, *92*, 5405. (b) Hopper, D. G.; Wahl, A. C.; Wu, R. L. C.; Tiernan, T. O. *J. Chem. Phys.* **1976**, *65*, 5474.

(9) Conrad, H.; Ertl, G.; Kuppers, J.; Latta, E. E. *Surf. Sci.* **1975**, *50*, 296.

(10) Oh, S. H.; Fisher, G. B.; Carpenter, J. E.; Goodman, D. W. *J. Catal.* **1986**, *100*, 360.

(11) Somorjai, G. A. *Introduction to Surface Chemistry and Catalysis*; John Wiley & Sons: New York, 1994.

(12) Root, T. W.; Schmidt, L. D.; Fisher, G. B. *Surf. Sci.* **1983**, *134*, 30.